THERMAL PROCESSES AND STABILITY OF A SUPERCONDUCTIVE DIPOLE MAGNET WITH PULSED HEATING OF THE WINDING

P. G. Vasilev, B. A. Vakhnenko, V. I. Deev,
L. N. Zaitsev, G. P. Reshetnikov,
A. E. Syreishchikov, and V. S. Kharitonov

UDC 536.24:537.312.62

Results of an experimental and numerical study of thermal processes occurring upon pulsed heating of the superconductive winding of a dipole magnet are presented.

It is well known that the superconductive windings of dipole magnets are subjected to impulsive radiation of varying duration due to particle loss. Thus, it becomes necessary to determine the maximum permissible levels of energy liberation which do not cause a transition of the winding to the normal state, and to study the dynamics of this transition. It should be noted that upon radiant energy liberation in a composite cable a transverse temperature gradient can develop, with formation of a limited normal zone as a consequence [1]. The appearance of such a zone can lead to perturbation of the field in the magnet system aperture and affect the dynamics of the accelerated particle beam [2]. Study of these questions is possible only by simultaneous use of computational and experimental methods.

In the present study the problem formulated will be solved for a "window frame" type superconductive dipole magnet [3, 4].

A cross section of a portion of the magnet winding is shown in Fig. 1. The winding is constructed of a plane transposed superconductive cable (dimensions 3.7 × 0.92 mm). The cable contains 15 composite niobium–titanium conductors (NT-50) with diameter of 0.5 mm. Internally the cable is wrapped with two layers of Lavsan film and a glass cloth layer, alternately wound. The cable's conductor packing coefficient is 0.93.

Heat liberation in the winding was simulated by pulsed heating of the cable with a special heater located between two turns of the winding. The heater was constructed of Constantan wire 0.35 mm in diameter with a resistance of 1.3 Ω, insulated by lacquer and a silk coating. Temperature field dynamics in the winding were tracked by type TVO and Allen-Bradley (AB) carbon resistance thermometers. The thermometers were attached to the surface of the cable with type BF-4 glue after insulation was removed and were thermally insulated from the surrounding medium by resin-impregnated glass cloth. The experimental magnet winding was placed in a cryostat with liquid helium in the saturated state at a temperature of T_l = 4.2°K.

The measurements of permissible energy liberation in the series of experiments performed in this study were carried out with constant standing current in the magnet winding. The heater was driven by brief (~0.5 msec) electrical pulses. The level of energy liberated in the heater was increased in fixed steps until the magnet winding shifted into the normal state. Then a new value of standing current was established in the winding and the measurements were repeated. The resistance thermometer readings were recorded simultaneously. A more detailed description of the apparatus and experimental technique is presented in [1].

Figure 2 shows the experimentally obtained dependence of permissible energy liberation in the heater Q as a function of the ratio of the magnet current I to the critical value I_{cr}. Here $I_{cr} \approx 2$ kA is the critical magnet winding current in the intrinsic magnetic field at a temperature of 4.2°K. The unfilled points on the graph correspond to energy values at which there is no transition to the normal state, while the filled points cause such a transition to occur.

Joint Institute for Nuclear Research, Moscow. Moscow Engineering Physics Institute.
Translated from Inzhenerno-Fizicheskii Zhurnal, Vol. 48, No. 2, pp. 301-305, February, 1985. Original article submitted December 15, 1983.

 0022-0841/85/4802-0224$09.50

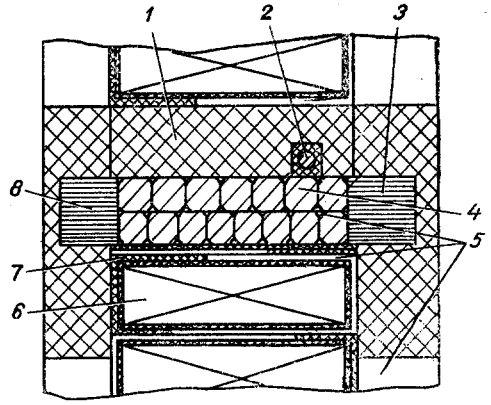

Fig. 1

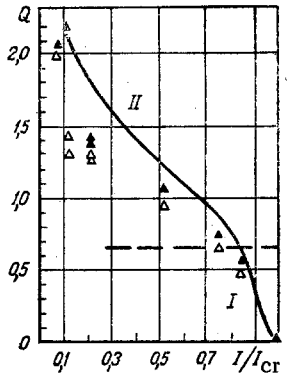

Fig. 2

Fig. 1. Cross section of experimental portion of magnet winding: 1) resin-impregnated glass cloth; 2) heater; 3) TVO thermometer; 4) NT-50 conductor; 5) liquid helium; 6) superconductive cable; 7) cable insulation; 8) AB thermometer.

Fig. 2. Maximum energy liberation in heater Q (J) vs standing current in "window frame" type dipole magnet winding: points, experimental data; curve, calculation. I/I_{cr} (T, B).

Figure 3 shows experimental curves of the heating $\Delta T(\tau) = T(\tau) - T_\zeta$ of the AB and TVO thermometers for two Q values, obtained in measurements in which the magnet did not transform to the normal state. It is evident that with identical energy liberations in the heater, the AB thermometer heats more rapidly than the TVO. This is apparently because the geometric dimensions and, thus, the thermal inertia of the AB thermometer are less than those of the TVO. However, the maximum temperature rise of the TVO is greater than that of the AB. This indicates that because of the asymmetric location of the heater, the face of the cable to which the TVO thermometer was attached reached a higher temperature in the heating process.

The temperature fields in the magnet winding were calculated for the experimental conditions by simulating heat transfer with a set of one-dimensional thermal conductivity equations for layers into which the calculated region was divided [5]. Four such layers were used in the region of the winding near the heater in the computational equivalent of the real geometry. The first layer simulates the heater and glass cloth layer; the second, the cable and resistance thermometer; the third, the helium held in the spaces between the cable conductors; and the fourth, the cable insulation. Thermal interaction between these layers and with adjacent turns of the cable and the helium located between cable turns was considered by introducing appropriate terms into the equations. The system of thermal conductivity equations obtained in this manner together with initial and boundary conditions was solved numerically. The number of calculation points chosen within the limits of each layer allowed proper consideration of layer inhomogeneity over length, as well as change in thermophysical properties of the materials with temperature. The calculations assumed that the fraction of helium in interstices was 7% of the cable volume.

To describe nonsteady-state heat transfer to the helium a model previously developed [6] was used. This model considers a sequence of heat-transfer regimes which occurs in time as a thermal load is imposed on a surface located within a large helium volume: nonsteady-state thermal conductivity regime, as well as nonsteady-state bubble and film boiling regimes. Under the conditions of the present experiment the quantity of heat transferred to the helium held in winding gaps was sufficient for its complete evaporation. This required appropriate changes in the calculation model, namely, consideration of degradation of heat transfer due to gradual evaporation of helium and accumulation of vapor in the interstices, as well as allowing for possible superheating of the vapor. To describe these processes it was assumed that the intensity of heat liberation begins to decrease as compared to heat liberation in a large volume at a vapor content in the spaces $\varphi > 0.5$, while at $\varphi = 1$ the heat liberation coefficient is determined by the thermal conductivity of the helium vapor layer.

In accordance with the experimental conditions, in performing the calculations a heat source was specified within the heater volume, varying with time by a law

$$q_v = q_v(0) \exp(-4 \cdot 10^3 \tau). \quad (1)$$

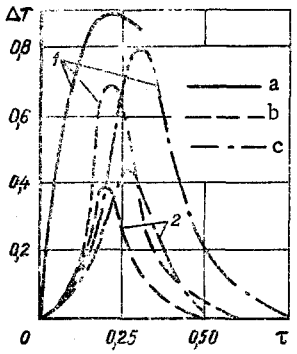

Fig. 3

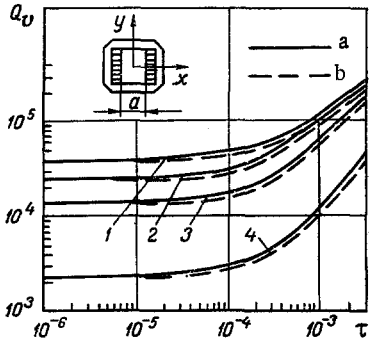

Fig. 4

Fig. 3. Calculated (a) and experimental curves of change with time τ (sec) of excess temperatures ΔT (°K) of AB (b) and TVO (c) thermometers: 1) Q = 1.08 J; 2) 0.61.

Fig. 4. Maximum permissible energy liberation Q_v (J/m³) vs pulse duration τ (sec) at E_p = 1 GeV for element with coordinates x = $a/2$, y = 0 (a) and winding as a whole (b): 1) I/I_{cr} = 0.2; 2) 0.4; 3) 0.6; 4) 0.9.

The temperature of calculation points within the winding element being considered was established at each step in time. Using the time dependence of cable temperature thus found T(τ), admissible energy liberation levels in the heater were found. To do this the maximum cable temperature values T_m for each heater power Q were used to calculate critical currents I_{cr} (T_m, B) in the magnet winding. This was done with the function $I_{cr} = I_{cr}(T, B)$ obtained from the characteristics of a short specimen of NT-50 wire with consideration of the critical current value of the experimental magnet at 4.2°K. It was assumed further that the amount of energy liberated in the heater Q was the maximum possible for a winding with standing current of I, if the equation $I = I_{cr}(T_m, B)$ was satisfied. The dependence of permissible energy liberation in the heater on standing current determined in this manner is shown by the solid line of Fig. 2. It is evident that the calculated values of permissible energy liberation coincide approximately with experiment. The numeral I denotes the range of Q values in which calculations indicate the magnet transforms to the normal state with nonsteady-state bubble and film boiling of the helium in the interstices, while II indicates the range of the vapor superheating regime (regions I and II are separated by a dashed line in Fig. 2).

The solid line of Fig. 3 is the calculated change with time of excess temperature of the TVO thermometer. The divergence between the maximum calculated and experimental values of ΔT does not exceed 10%. The shift of the curves with time is apparently related to indefiniteness of the resistance thermometer inertial characteristics under the experimental conditions, which could not be considered properly in the calculations. It should be noted that calculations of the process with assumption of absence of helium from the spaces between conductors produce great divergence from experiment.

At Q = 1.3 J temperature nonuniformity over cable cross section was calculated to be ~0.1°K.

On the whole, satisfactory agreement of calculated and experimental data permitted use of the calculation method developed to determine permissible radiant energy liberation in a "window frame" type magnet, caused by loss of 1-GeV protons. The heat-transfer processes in the winding were modeled in the above manner. It was assumed that energy liberation occurred at the initial moment with specific power distributed uniformly over magnet length and normally over the y coordinate (see inset of Fig. 4):

$$q_v = 1.2 \cdot 10^{-6} E_p L \exp[-y^2/2\sigma_y^2 - \gamma(E_p)\sqrt{(1+4y^2/a^2)(x-a/2)}], \quad (2)$$

where $\gamma(E_p) = 3.1 \ln E_p + 4.1$ ($m^{-1/2}$).

Equation (2) was obtained on the basis of data from [7] on the distribution of energy density over winding thickness for loss of protons with energies of 1-1000 GeV.

The solid lines of Fig. 4 show the calculated values of specific energy liberation necessary for transition to the normal state of an element of the winding with coordinates x = $a/2$, y = 0 as a function of pulse duration for various values of the ratio of standing current to

critical current. The dashed line is the energy level necessary for transition of the winding as a whole to the normal state (the normal zone occupies the entire cable cross section). It is evident that for a fixed energy liberation a certain time interval exists between the transitions to the normal state of the element with coordinates $x = a/2$, $y = 0$ and the winding as a whole.

NOTATION

a, distance between the magnet semiwindings, m; B, magnetic induction, T; E_p, proton energy; I, current, kA; L, number of lost protons per unit magnet length, m^{-1}; Q, energy, J; Q_V, specific energy liberation per unit volume, J/m^3; T, temperature, °K; ΔT, excess temperature, °K; x, y, coordinates; σ_y, dispersion of the normal distribution, m; τ, time, sec; φ, vapor content. Subscripts: l, liquid helium; cr, critical; m, maximum.

LITERATURE CITED

1. P. G. Vasilev, A. M. Donyagin, I. A. Eliseeva, et al., "Measurement of field inhomogeneity under conditions of pulsed heating of a superconductive magnet winding," Joint Institute for Nuclear Studies Report R9-83-394 [in Russian], Dubna (1983), pp. 1-12.
2. P. G. Vasilev, L. I. Greben', L. N. Zaitsev, et al., "Effect of beam energy loss on particle dynamics in superconductive synchrotrons," Joint Institute for Nuclear Studies Preprint R9-82-486 [in Russian], Dubna (1982), pp. 1-12.
3. E. P. Zhidkov, R. Ya. Polyakova, and I. A. Shelaev, "Magnetic field calculation in 'window frame' type superconductive dipoles," Joint Institute for Nuclear Research Report R11-12324 [in Russian], Dubna (1979), pp. 1-12.
4. I. A. Shelaev and I. P. Yudin, "Study of two-dimensional superconductive dipole magnetic fields by the conjugate current method," Joint Institute for Nuclear Research Report R9-80-333 [in Russian], Dubna (1980), pp. 1-13.
5. I. G. Merinov, "Method of calculating temperature fields in a superconductive magnet system with local impulsive thermal perturbation," in: Computational-Theoretical and Experimental Studies in Nuclear Reactor Thermophysics [in Russian], Énergoatomizdat, Moscow (1983), pp. 36-40.
6. B. A. Vakhnenko, V. I. Deev, Yu. A. Kuz'min, and V. S. Kharitonov, "Calculated model of nonsteady state heat transfer to liquid helium with impulsive heating," in: Computational Theoretical and Experimental Studies in Nuclear Reactor Thermophysics [in Russian], Énergoatomizdat, Moscow (1983), pp. 31-36.
7. L. N. Zaitsev, "The problem of superconductive magnet stability in accelerators with irradiation by high-energy particles," Fiz. Element. Chast. At. Yad., 11, No. 3, 525-570 (1980).